

# N-cadherin modified lipid bilayer promote neural network formation and circuitry

K. Zobel,<sup>a</sup> S.E. Choi,<sup>a</sup> R. Minakova,<sup>a</sup> M. Gocyla,<sup>a</sup> A. Offenhäusser<sup>a,†</sup>

Received 00th January 20xx,  
Accepted 00th January 20xx

DOI: 10.1039/x0xx00000x

www.rsc.org/

Neural adhesion, maturation, and the correct wiring of the brain to establish each neurons' intended connectivity are controlled by complex interactions of bioactive molecules such as ligands, growth factors, or enzymes. The correct pairing of adjacent neurons is thought to be highly regulated by ligand-mediated cell-cell adhesion proteins, which are known to induce signaling activities. We developed a new platform consisting of supported lipid bilayers with incorporated Fc-chimera synaptic proteins like ephrinA5 or N-cadherin. We extensively characterized their function employing a quartz crystal microbalance with dissipation (QCM-D), calcium imaging, and immunofluorescence analysis. Our biomimetic platform has been shown to promote neural cell adhesion and to improve neural maturation at *day in vitro* 7 (DIV7) as indicated by an elevated expression of synaptophysin.

## 1. Introduction

The orientation and polarization of neurons in the developing brain play an important role for the correct wiring. Specifically, the formation of axo-dendritic domains are crucial events to form functional synapses. In these events, cell adhesion proteins play a substantial role in cell differentiation, guidance, and communication mediated by signaling cascades and trans-cellular communication. At the level of axo-dendritic contacts, synaptogenesis is initiated by specific adhesion proteins including Ephrins (ephrinA5), Cadherins (N-cadherin), Neurexins, Neuroligins, SynCAMs, and leucine-rich repeat transmembrane molecules (LRRTMs).<sup>1–3</sup> Nevertheless, the structural remodeling of the spines is a dynamic process and is highly dependent on the type of synapse and changes in various stimuli or synaptic activity.<sup>4</sup> Among adhesion proteins, ephrinA5 and N-cadherin are critically involved in numerous biological processes, such as neuronal adhesion and guidance.<sup>5</sup>

Ephrin ligands and their equivalent receptors are divided in two major classes, A and B,<sup>6</sup> which differ by their mode of attachment to the plasma membrane. While ephrin A ligands are tethered to the cell membrane by virtue of a glycosylphosphatidylinositol (GPI) anchor, ephrin B ligands are structurally characterized as transmembrane proteins. Ephrin receptors (EphrA) consist of a unique cysteine rich domain with a fibronectin-III (FNIII) motif and a tyrosine kinase activity.<sup>7</sup> Despite their structural diversity, the ephrinA ligands cluster on the cell membrane in distinct microdomains, known as lipid rafts or caveola-like domains, that are characterized by their unique compositional enrichment of glycosphingolipids.<sup>8</sup> Structure and sequence homology analysis have shown that pairs of Eph receptors and ephrin ligands differ in each subclass. Whereas eight different EphrA receptors interact with five ephrinAs, six EphrB receptors interact with three ephrinBs.<sup>6</sup> As a critical ligand in early neural development, ephrinA5 has been shown to increase cell adhesion and influence neuronal guidance,<sup>9</sup> migration, and differentiation.<sup>10</sup> Receptor-ligand studies have shown

that the phosphorylation and activation of signal cascades require a clustering of ephrin molecules.<sup>11</sup>

Besides ephrinA5, N-cadherin is a transsynaptic adhesion protein which mediates adhesive roles and signal propagation in neurons,<sup>12</sup> stimulates spine heads over long periods of time,<sup>13</sup> and regulates the stabilization of spines<sup>14</sup> over long time scales. Furthermore, Okada et al. have shown that N-cadherin is preferentially recruited to activated synapses.<sup>15</sup> Here, the intracellular signaling and modulation of the actin cytoskeleton is mainly driven by a large variety of intracellular signal molecules.<sup>16</sup> The modular structure of cadherin encompasses five tandemly repeated similar domains of ~110 amino acids each. The specific homophilic binding between cadherins then occurs through interaction of the N-terminal domains (Figure 1C). Here, cations, such as Ca<sup>2+</sup>, coordinate the successive domains to rigidify the multidomain molecule.<sup>17</sup> Receptor-ligand studies in the ephrin and cadherin signaling systems are of increasing importance. Not only do we need a system to specifically discriminate the impact of ephrinA5 and N-cadherin during the development of neural networks, but studies of the interaction between synaptic adhesion proteins and the cell membrane must retain the functional and structural properties of the adhesion proteins. In particular, since protein clustering is necessary for phosphorylation and subsequent signal cascades, the mobility of the proteins of interest must be maintained. EphrA receptors, for example, induce signal cascades by forming specific caveola-like domains. In order to allow this mobility and conserve the orientation of membrane proteins, supported lipid bilayers (SLBs) have been prepared on substrates such as glass or silica and extensively used as a model system to study cell-cell and cell-membrane interactions.<sup>18</sup>

Particularly, SLBs facilitate the proper assembly of membrane protein clusters by maintaining free lateral diffusion of the protein, with a thin layer of water trapped between the solid support and the bilayer.<sup>19–21</sup> As a consequence, SLBs have become a convincing model system to mimic natural membranes in the last decades,<sup>22</sup> with this artificial membrane initially replacing an adjacent cell or synaptic component. The use of protein-modified SLBs is of high relevance to provide the closest alternative to a natural membrane. Presently, cell adhesion proteins can be incorporated into SLBs using different methods to establish an artificial protein-doped membrane,<sup>23</sup> either via GPI-linkers employed to tether proteins to the membrane,<sup>24,25</sup> 6-

<sup>a</sup> Institute of Bioelectronics (ICS-8), Forschungszentrum Juelich, Wilhelm-Johnen

Straße, 52425 Juelich, Germany

† corresponding author

Electronic Supplementary Information (ESI) available

See DOI: 10.1039/x0xx00000x

histidine (6-His) tag-modified proteins attached to Ni<sup>2+</sup> chelating phospholipids,<sup>26</sup> or proteins linked to biotinylated phospholipids via biotin-streptavidin binding.<sup>27</sup>

In the present study, we propose an approach to integrate Fc-chimera-conjugated synaptic adhesion proteins into lipid bilayers to mimic a natural synaptic unit. The Fc-part of the conjugated protein acts as an anchor for incorporation of the adhesion protein into the bilayer membrane. N-cadherin and ephrinA5, as known modulators of synaptic modulation, have been produced as recombinant, SLB incorporable chimeras, and used in synthetic 1-palmitoyl-2-oleoyl-sn-glycero-3-phosphocholine (POPC) SLBs. The ephrinA5 Fc-chimera is characterized by two ephrinA5 molecules coupled to the Fc domain, whereas Fc-modified N-cadherin proteins consist of one mature cell surface domain that contains five cadherin repeats attached to one Fc domain. In this research, we show that the incorporation of Fc-modified synaptic adhesion proteins into SLBs can expose accessible domains to neuronal receptors, while preserving the function and structural properties, such as clustering, required of ephrinA5 proteins. The embedding of proteins of interest in SLBs is an efficient *in vitro* model to precisely characterize their individual effect on neural maturation and development. In this context, we could show that N-cadherin-doped artificial membranes increase neural polarity already at *day in vitro* 1 (DIV1) by a faster outgrowth of neurites, in contrast to an ephrinA5 modified lipid bilayer. Here, calcium imaging analyses and immunofluorescence analyses suggest a higher expression of synaptophysin for neurons already at DIV7 on N-cadherin doped SLBs.

## 2. Experimental

### 2.1 Materials and Instruments

The Avanti mini Extruder, polycarbonate membranes (1.0 µm, 19 mm (100/pk)), filter support membranes, the lipid POPC (1-palmitoyl-2-oleoyl-sn-glycero-3-phosphocholine) at 20 mg/mL in chloroform, and the detergent in powder form of n-octyl-β-D-glucopyranoside (NOG), were purchased from Avanti Polar Lipids. The labeled lipids Texas Red 1,2-dihexadecanoyl-sn-glycero-3-phosphoethanolamine, triethylammonium salt (Texas Red DHPE), and OregonGreen 1-oleoyl-2'-sn-glycero-3-phosphoethanolamine (NBD-PE) were obtained from Invitrogen GmbH. EphrinA5 (recombinant Human ephrinA5 Fc-Chimera, CF), N-cadherin (recombinant Human N-cadherin Fc-Chimera, CF), the primary antibody goat anti-human ephrinA5 (incorporated ephrinA5 receptor), and the primary antibody goat anti-human N-cadherin (incorporated N-cadherin ligand) were purchased from R&D Systems, whereas the mouse anti-ephrinA5 antibody (ligand), mouse anti-N-cadherin, mouse anti-Synaptophysin (7H12) and rabbit anti-Tubulin beta 3 (TUJ1; D71G9) were purchased from Cell Signaling Technology. Alexa Fluor 350 donkey anti-mouse IgG (H+L), Alexa Fluor 488 donkey anti-goat IgG (H+L), Alexa Fluor 546 rabbit anti-mouse IgG (H+L), Alexa Fluor 633 goat anti-rabbit IgG (H+L), and Alexa Fluor 488 donkey anti-mouse IgG (H+L) were from Life Technologies. DyLight microscale antibody labeling kits (DyeLight™, AlexaFluor 546), as well as Fluo-4 AM for calcium imaging were obtained from Thermo Scientific. Neurobasal medium, B27 supplement, L-Glutamine, and Dulbecco's phosphate buffered saline (DPBS) were purchased from Invitrogen. Gentamicin, trypan blue (0.4% solution), laminin for surface coating, and poly-D-lysine (PDL) were purchased from Sigma Aldrich GmbH. Hellmanex III for cleaning coverslips was obtained from Hellma Analytics. For calcium imaging analysis image sequences were acquired with a Zeiss Observer.Z1 equipped with a Zeiss Colibri

system and a PCO.edge 5.5 scientific complementary metal-oxide-semiconductor (sCMOS) camera with 1280 x560 pixels.

### 2.2 Surface preparation

Ibidi® 35 mm µ-Dishes with a high glass bottom (ibidi GmbH) were used as substrates for the characterization of lipid bilayer formation with an AxioScope from Carl Zeiss GmbH, immunofluorescence imaging, and MatLab analysis of calcium imaging data. Ibidi® dishes were cleaned with 100% isopropanol for 5 min, were extensively cleaned by rinsing with MilliQ water ten times and dried in a stream of nitrogen. The cleaned glass bottoms were activated by oxygen plasma in a Pico plasma system (Diener Electronics) for 5 min at 0.4 mbar and 80 W generator power immediately prior to bilayer preparation. Afterwards, ibidi® dishes were sterilized by UV for 1h.

### 2.3 Bilayer preparation and characterization

Proteoliposomes were prepared by detergent-mediated reconstitution. For this, labeled lipids and POPC were mixed. The final concentration of fluorescently labeled lipids in POPC was 1% (w/w). POPC was dried in a stream of nitrogen onto the walls of a glass vial and then left in vacuum for 1h to remove solvent residues. The detergent-pretreated protein solution was added to the dried lipids to get a final concentration of 12 mM NOG and 6 µg/mL of recombinant human ephrinA5 or N-cadherin Fc-chimera in 100 mM Dulbecco's phosphate-buffered saline (DPBS). The final POPC concentration was 1 mg/mL. Subsequently, the lipid solution was mixed by vortexing for 1 min and sonicated for 45 min on ice. Afterwards, the solution was extruded 20 times through a 100 nm polycarbonate membrane using an Avanti mini Extruder to form small unilamellar vesicles (SUVs). To form the supported lipid bilayer (SLB), the vesicle solution was diluted to 0.3 mg/mL with sterile DPBS and a total volume of 1 mL of the proteoliposome solution was added to the glass surface for at least 45 min at room temperature (RT) or overnight at 4°C covered with a final concentration of 12 mM NOG and 6 microgram per milliliter of recombinant human ephrinA5 or N-cadherin Fc-chimera in 100 mM DPBS. Residual unbound SUVs and NOG were removed with a stream of DPBS using a syringe (3 mL of PBS per ibidi® dish). Prior to cell plating, the PBS was refreshed and exchanged for cell culture medium (neurobasal medium) without exposing the lipids to air.

### 2.4 Characterization of lipid bilayer by QCM-D

Lipid bilayer formation was monitored by a quartz crystal microbalance with dissipation (QCM-D, Q-sense, Västra Frölunda, Gothenburg, Sweden). The lipid vesicle solution (1 mL) diluted to 0.3 mg/mL in DBPS (from Sigma Aldrich) together with 12 mM NOG and 6-12 µg/mL of ephrinA5-Fc/N-cadherin-Fc were deposited onto the SiO<sub>2</sub>-coated sensor surface in a QCM-D open module. After lipid bilayer formation, remaining lipid vesicles were rinsed away with PBS. Bilayer formation with vesicle solution and 12 mM NOG (without protein) was also monitored as a control experiment.

### 2.5 Protein-antibody binding measurement with QCM-D

Lipid bilayers were prepared on SiO<sub>2</sub> coated sensors. After approximately 60 min incubation time, primary goat anti-ephrinA5 or mouse anti-N-cadherin antibodies were applied to the SLBs. The incubation of the antibodies was carried out until the frequency

signal remained constant. Residual antibody was removed by rinsing the lipid membranes with PBS. The change in mass during the incubation process was calculated by the Sauerbrey equation,

$\Delta m = -\frac{C \cdot \Delta f}{n}$  (1) where  $\Delta m$  is the change in mass,  $\Delta f$  the change in frequency,  $C$  is the Sauerbrey constant of the material (17.7 ng/Hz cm<sup>2</sup>), and  $n$  is the overtone. The use of the Sauerbrey equation was possible due to a constant  $\Delta f/n$  ratio and a very low change in dissipation ( $\Delta D$ ) in all cases, indicating that the SLBs behave as a rigid system on the QCM-D.

## 2.6. Preparation of poly-D-lysine on plasma-activated glass

Control substrates were coated with the synthetic cell adhesive cationic polymer, poly-D-lysine (PDL). PDL was diluted in bidistilled water to a concentration of 10 µg/mL and incubated on the plasma-activated glass surface overnight in a humidified 5% CO<sub>2</sub> atmosphere at 37°C. Before cell plating, the PDL solution was removed and substrates were re-coated with 2 µg/mL of laminin for 30 min at 37°C in a humidified 5% CO<sub>2</sub> atmosphere. Both PDL and laminin were obtained from Sigma Aldrich.

## 2.7. Labeling of N-cadherin- and ephrin-Fc-chimeras with DyLight™

The labeling of ephrinA5 and N-cadherin chimeras was carried out with the commercially available DyLight™ Microscale Antibody Labeling Kit according to the manufacturer's instructions. The lyophilized proteins were diluted to a final concentration of 1 mg/mL in 0.05 M borate buffer. 100 µL of the protein solution was transferred to the DyLight reagent vial and was incubated in the dark for 1 hour at RT. After activating the spin column by Purification Resin to ensure a uniform suspension, the reaction mixture was deposited and centrifuged for 1 min at ~1000 × g to collect the purified labeled protein.

## 2.8. Cell adhesion studies on SLBs

### 2.8.1. Neuronal cell culture

Rat embryonic cortical neurons were isolated as described elsewhere.<sup>29</sup> Briefly, embryonic cortices were removed from pregnant Wistar rats at 18 days gestation (E18) and stored in Hank's balanced salt solution without Ca<sup>2+</sup> and Mg<sup>2+</sup>, supplemented with 1 mM sodium bicarbonate, 1 mM sodium pyruvate, 10 mM HEPES and 20 mM Glucose (HBSS-) (Sigma Aldrich). Dissected cortices were dissociated with a silanized, fire-polished pasteur pipette in 1 mL HBSS-. After dissociation, two volumes of HBSS+ (with Ca<sup>2+</sup> and Mg<sup>2+</sup> and supplements) were added to the cell suspension. The suspension was incubated on ice for 3 min to facilitate the sedimentation of clustered cells. The top half of the suspension was collected and centrifuged for 2 min at 200 g. After centrifugation, the cells were resuspended in neurobasal medium with 1% B-27 (Gibco, Grand Island, NY, USA), 0.5 mM glutamine, and 50 µg/mL gentamicin. Live cells were counted using trypan blue staining and a Neubauer chamber. 100,000 cells per 35 mm ibidi-dish were plated either on SLB-coated or control samples with PDL and laminin coating as described above. Three hours after cell plating, the medium was replaced with 2 mL of fresh medium. For every subsequent medium change, half of the medium was exchanged with fresh medium. The samples were kept at 37°C, 5% CO<sub>2</sub>, and 100% humidity.

Furthermore, glass substrates coated with ephrinA5 or N-cadherin were used as controls. Here, ephrinA5-Fc or N-cadherin-Fc was applied to clean glass coverslips and incubated for 30 min at RT. To remove unbound proteins, the surface was washed with PBS before plating neurons.

### 2.8.2. Phase contrast and immunofluorescence analysis

The neurite outgrowth of cortical neurons from DIV1 until DIV14 was studied by phase contrast microscopy. Protein expression analysis of synaptic proteins such as synaptophysin was verified by immunofluorescence microscopy (Zeiss AxioScope, CarlZeiss GmbH). Briefly, cells were fixed with 4% paraformaldehyde in PBS for 20 min at RT and washed with PBS thrice. Unspecific binding sites were saturated with 1% BSA and 2% goat serum in PBS (blocking buffer). The cell membrane was permeabilized by 0.01% Triton X-100 in blocking buffer for 20 min at RT. Samples were washed with PBS twice and then incubated with the primary antibodies overnight at 4°C. Mouse anti-Synaptophysin, mouse anti-ephrinA5-Ab, or mouse anti-N-cadherin were used at 1:200 dilution in blocking buffer. After washing with PBS, secondary antibodies, as listed above, were applied for 1 h at a dilution of 1:500 in blocking buffer at RT. After incubation, the samples were rinsed with PBS and stored in PBS for the subsequent microscopic observation. Cells were visualized with a Zeiss Colibri system and a PCO.edge 5.5 sCMOS camera.

### 2.8.3 Calcium imaging analysis

Calcium imaging was employed to visualize and measure spontaneous neuronal activity on the substrates. Neurons were cultured for 7 to 14 days *in vitro* on SLBs in ibidi-petri dishes. For calcium imaging experiments, the osmolarity of the culture medium was determined to enable a matching of the employed E-patch buffer (Osmomat 3000, GONOTEC GmbH). In cases where the osmolarity of the culture medium exceeded the osmolarity of E-patch buffer by more than 20 mOsmol/kg, the osmolarity of the E-patch solution was adjusted to match the value of the medium directly before the experiment with D-(+)-glucose (Sigma Aldrich). E-patch contains: 2 mM CaCl<sub>2</sub>, 10 mM HEPES, 3 mM KCl, 1 mM MgCl<sub>2</sub>, 120 mM NaCl; the pH of the solution was adjusted to 7.3 with 1M NaOH. For the measurement, samples were washed once with pre-warmed E-patch solution. To visualize neuronal activity optically, the cells were incubated with 4 mM Fluo-4 AM (Invitrogen) in E-patch for 45 minutes in the dark at RT. Unincorporated Fluo-4 was removed by rinsing with E-patch twice, being careful to avoid exposure of the lipids to air during the procedure. A final volume of 2 mL of E-patch solution was added to the substrate and an additional incubation time of 10 minutes in the dark at RT was applied. To achieve a maximal excitation of the dye, 70% intensity of the Colibri Light Emitting Diode (LED) ( $\lambda = 470$  nm) was chosen. Time sequences with a length of 1 s were recorded with the Zeiss ZEN blue software at an exposure time of 10 ms. A 2 × 2 binning was applied to the 1.3 µm pixels, and the active area of the sensor was reduced to 1280 × 512 pixels resulting in an imaged area of 1.66 mm × 0.666 mm with a resolution of 2.6 µm.

## 3. Results and discussion

Cell-substrate interactions and the resulting influence on cellular signal cascades are of high importance for neuronal cells. In this

study, we introduce a system focusing on cell adhesion to artificial membranes for *in vitro* applications. Here, we incorporate human recombinant Fc-coupled proteins into supported lipid bilayers to preserve their natural functions and correct orientation (Figure 1).

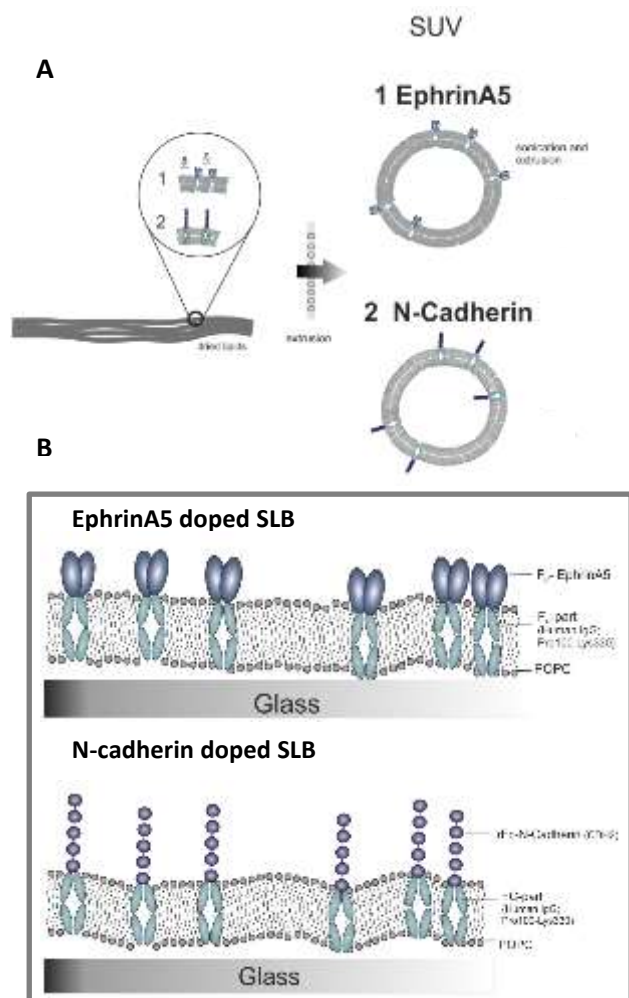


**Figure 1: Reconstitution of recombinant Fc-chimera synaptic adhesion proteins in a fluid lipid bilayer (POPC).** A) Schematic of the reconstitution of ephrinA5 and N-cadherin into small unilamellar vesicles (SUVs) and B) formation of lipid bilayer (POPC) after sonication and extrusion (100 nm polycarbonate membrane).

### 3.1. SLB characterization

Recombinant human ephrinA5-Fc or N-cadherin-Fc were incorporated into small unilamellar vesicles (SUVs) consisting of 1-palmitoyl-2-oleoyl-sn-glycero-3-phosphocholine (POPC) by a detergent-mediated procedure.<sup>30,31</sup> Prior to the proteoliposome formation, human recombinant proteins were labeled by DyLight™ and were mixed with with n-octyl-β-D-glucopyranoside (NOG). Subsequently, labeled adhesion proteins were mixed with dried lipids after evaporation. A small amount of the fluorescently labeled lipid 1,2-dihexadecanoyl-sn-glycero-3-phosphoethanolamine, triethylammonium salt (Texas Red DHPE) or 1-oleoyl-2-sn-glycero-3-phosphoethanolamine (NBD-PE) was added to visualize and prove the formation of artificial membranes. Subsequently, small unilamellar N-cadherin-Fc- or ephrinA5-Fc-doped vesicles were extruded (Figure 1, A) and deposited on activated glass surfaces of ibidi-dishes (Figure 1, B). The formation of SLBs and the incorporation of human recombinant proteins were analyzed by QCM-D

measurements (Figure 2). We monitored the formation of the POPC bilayer with incorporated N-cadherin on a SiO<sub>2</sub> coated sensor. The formation of ephrinA5 containing SLBs formation was evaluated by Ghosh Moulick et al.<sup>32</sup>

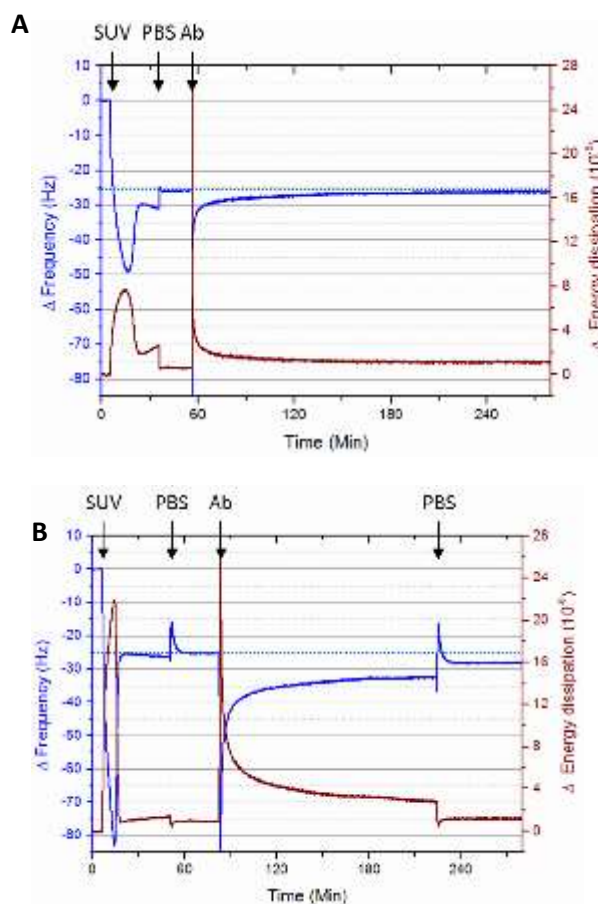


**Figure 2: QCM-D response of anti-N-cadherin antibody binding on the protein doped lipid bilayer.** QCM-D response of anti-N-cadherin antibody binding on the protein doped lipid bilayer. POPC lipid bilayers were made either without NOG (A) or with NOG (B) on SiO<sub>2</sub> coated sensors. When SUVs were introduced on the SiO<sub>2</sub> surface, they adsorbed on the sensor until the critical concentration was reached and they started to rupture. After bilayer formation, excess vesicles were removed by PBS and anti-N-cadherin antibodies were applied (Ab). Here, N-cadherin antibodies bind to the SLB only when NOG was used in combination with N-cadherin, as can be seen from the shift to more negative frequency values (Δf). According to the Sauerbrey equation, this frequency change signifies increase in mass and thus indicates antibody only binds to SLB. They show that NOG is necessary to incorporate proteins into SLB.

A change in mass (Δm) on the sensor surface is proportional to the change of the resonance frequency (Δf), according to the Sauerbrey relation (see Equation 1). With the change in energy dissipation (ΔD) we could evaluate the change of frictional (viscous) loss stemming from the viscoelastic properties of SLB<sup>33</sup>. When lipid vesicles are injected onto the SiO<sub>2</sub> sensor surface, vesicles adhere to the sensor surface. Vesicles start to rupture once they have reached the critical concentration on the surface which is shown as the lowest Δf and highest Δm before bilayer formation. Characteristic QCMD signal of bilayer formation is Δf of approximately 24.5 Hz and ΔD of around 0. Proteoliposomes also reach critical concentration on the SiO<sub>2</sub> surface before rupture and bilayer formation. After the formation of the bilayer, PBS washing removed unruptured proteoliposomes on the bilayer easily, which resulted in increase in frequency shift and

decrease in dissipation shift. The presence of the ephrinA5 or N-cadherin domain on the SLB was verified via the binding of antibodies to the surface. The amount of bound antibody on the bilayer can be calculated from the frequency change after the application of the antibody (Fig. 2 B,  $\Delta f \approx 2.8$  Hz), via Equation (1). Assuming one antibody binds only on protein, and the molecular weight of one antibody is 160 kDa, the amount of protein in the bilayer is about 49.56 ng/cm<sup>2</sup>  $\approx$  310 fmol/cm<sup>2</sup>. The mass of lipid in the SLB is around 440 ng/cm<sup>2</sup> ( $\Delta f \approx 24.5$  Hz, as can be seen in Fig. 2.A) and the molecular weight of POPC lipid molecules is about 760.1 g/mol, giving the number of POPC molecules approximately 570 pmol/cm<sup>2</sup>. Thus, the molecular ratio between lipid and antibody, and presumably lipid to N-cadherin, is around 1800:1, with is similar to the reported distribution and amount of ephrinA5 in the bilayer reported previously.<sup>32</sup> The orientation of the extracellular domain in the lipid bilayer and the accessibility of the Fc-par at the C-terminal end of SLB incorporated proteins was also reported in previous report using ephrinA5.<sup>32</sup>

The detection and localization of ephrinA5 or N-cadherin in artificial membranes has been confirmed by labeling with DyLight (660nm) (S 1, B and C, Supplementary Information), whereas pure and untreated POPC membranes show only the fluorescence of labeled lipids stained by Texas Red DHPE (S 1, A). Fluorescence analysis has shown that the lipid bilayer formation occurs after 30 min incubation. Fluorescently labeled TexasRed DHPE or fluorescently labeled incorporated ephrinA5-Fc or N-cadherin-Fc proteins have been detected after lipid bilayer formation.

### 3.2. Neuronal network formation and maturation on ephrinA5- and N-cadherin-doped artificial membranes

During neuronal network formation and maturation, cells break their symmetry and start the progression of polarization and axon differentiation. The process consists of five phases during which one of the neurites starts to differentiate into an axon. Synaptic proteins such as N-cadherin and ephrinA5 have been shown to be responsible for determining axonal neurite growth in developing neurons.<sup>10,11,14</sup> For example, N-cadherin induces the breakage of cell symmetry in pyramidal excitatory neurons.<sup>7</sup> To evaluate the relevance of both proteins with regard to the enhancement of neural network formation, phase contrast microscopy has been employed to determine the neurite length on protein-modified lipid substrates. The neuronal outgrowth was compared to control conditions such as the polycationic polymer Poly-D-Lysine (PDL) as a commercially available, strongly adhesive polymer that promotes cell adhesion, as well as to untreated glass surfaces and POPC. POPC lipid membranes have been shown to act as cell repellent (S2, Supplementary Information) and are used as control condition to prevent any cell adhesion.

In this study, cortical neurons were cultivated on PDL+laminin, N-cadherin- or ephrinA5-doped SLBs to promote cell adhesion and network formation (Figure 3, A). Cortical neurons on plasma-activated glass surfaces show only weak adhesion (S3, Supplementary Information). The use of PDL+laminin substrates yields good cell adhesion and neuronal network formation at DIV7 and DIV14 (Figure 3 A, (i-ii)). Neuronal cells cultured on N-cadherin-doped lipid membranes showed improved adhesion, with a homogenous cell distribution and neurite outgrowth until at least DIV14 (Figure 3 A, (iii-iv')) as compared to both PDL+laminin-coated substrates and ephrinA5-modified lipid bilayers (Figure 3 A, (vi)). EphrinA5 lipid membranes initially support adequate cell adhesion,

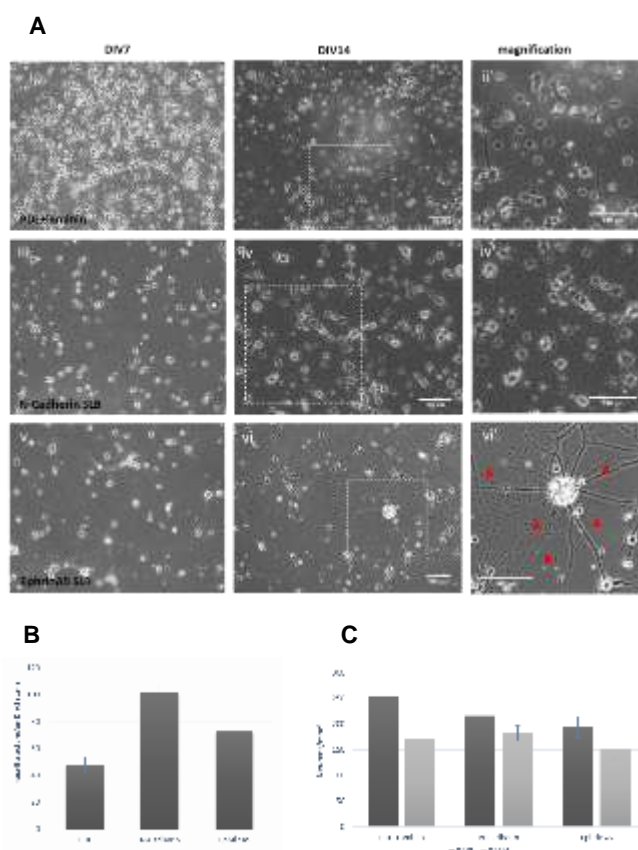


**Figure 3: Neuronal adhesion on modified lipid bilayer and PDL+laminin coated substrates.** **A)** Overview of neuronal adhesion on PDL+laminin (i, ii), N-cadherin-doped bilayer (iii, iv'), and ephrinA5-doped lipid bilayer (v, vi') (red arrows indicate degenerated neurites) at DIV7 and DIV14. Neurons on PDL+laminin (i, ii) show strong cell adhesion to the surface at DIV7 and DIV14, adhesion on N-cadherin bilayer at DIV7 and DIV14 shows homogenous distribution of neuronal cells while adhesion on ephrinA5 bilayers leads to cell aggregates both at DIV7 and DIV14. **B)** Determination of neurite length of cortical neurons on PDL+laminin coated surfaces and N-cadherin and ephrinA5 lipid bilayer at DIV1. **C)** Quantification of neuronal cell growth and number of live cells at DIV7 and DIV14 on various substrates.

however, the cells later undergo an aggregation with shortened neurites at DIV7. At DIV14, cell clusters could be observed on ephrinA5 lipid membranes, which are characterized by a further retraction (Figure 3 A, (vi')) (red arrows indicate the loss of synaptic connection by degrading neurites). Here, a strong destabilization of synaptic connections to adjacent neurons could be observed at DIV14.

To analyze the different influence on neuronal network formation we investigated and compared the role of N-cadherin and ephrinA5 on developing neurites (Figure 3 B). In pyramidal neurons, polarization begins with the sprouting of opposite neurites.<sup>34</sup> Our *in vitro* study has shown that the use of adhesion proteins in lipid substrates induces neural induction differently. To analyze if the neural polarity is specifically triggered by N-cadherin, dissociated cortical neurons were seeded on N-cadherin or ephrinA5 doped SLBs and their neurite outgrowth was compared with the highly attractive coating PDL+laminin. Neural sprouting and the length of the first neurites were determined at DIV1. We could show that the neurite length of cortical neurons on PDL+laminin is about 40 μm. In contrast to PDL+laminin, neurons on N-cadherin lipid bilayer show a neurite extension of about 100 μm at DIV1. Gärtner et al. found that the determination of the first neurite's outgrowth is determined by N-

cadherin localization after cell division. An increased concentration of N-cadherin at one pole of the neuron is likely to determine the location of the first neurite. Organelles, such as the Golgi apparatus and centrosome, are then relocated to this position.<sup>35</sup> We assume that the local stimulation by extrinsic N-cadherin adhesion proteins defines the pole of initial neurite outgrowth and enhances the neurite sprouting compared to PDL+laminin-coated substrates or ephrinA5 lipid bilayers.

Naturally occurring ephrinA5, a well-known cell-surface adhesion protein, is tethered to the cell surface, binds to EphrA tyrosine kinases and controls guidance cues in the developing nervous system.<sup>36</sup> These cues can be interpreted by the cells as attractive or repulsive, depending on downstream signaling events. Our observations have shown that cortical neurons cultured on ephrinA5-doped lipid membranes initially extend their neurites to a length of about 70  $\mu\text{m}$ . However, after initial cell-surface attachment, cell aggregation and neurite contraction could be observed in our study. We assume that cortical neurons on ephrinA5 lipid bilayers attach to ephrinA5 ligands, which dimerize and activate downstream axonal stimulating signals to favor initial axonal outgrowth. However, we suppose that higher-affinity interactions between the ephrinA5 and EphrA lead to a contact-mediated repulsion. Our assumption is based on studies from Marson et al. and Zimmer et al. who reported that destabilization of cell contact points and synapses is due to an upregulation of ephexin, a G-protein coupled factor.<sup>37,38</sup> Our results indicate that cortical neurons show a different adhesion behavior on different soft material. The cells show a stronger adhesion behavior on N-cadherin as compared to ephrinA5-doped SLBs or on immobile substrates such as PDL+laminin

at DIV7 (Figure 3 C). Cortical neurons cultured on PDL+laminin and N-cadherin substrates show a homogenous distribution and good adhesion in contrast to cells cultured on ephrinA5 lipid bilayers, which show cell aggregation already at DIV7. The number of viable neurons on PDL+laminin decreases at a higher rate from DIV7 to DIV14 as compared to N-cadherin or ephrinA5 lipid bilayers. The decrease in the number of neurons at DIV14 on different substrates is due to a reduction of contact points over culture time. In contrast, neurons do not grow on POPC lipid bilayers and just show a weak adhesion on glass surfaces (S2 + S3, Supplementary Information), confirming that the functional activation is mediated by receptor-ligand or ligand-ligand interactions. Furthermore, we assume that the neurite sprouting is not determined by adhesive strength, as shown for PDL+laminin, but critically depends on the adhesive specificity of the employed proteins and the fluidity of the lipid substrate. Additionally, N-cadherin increases the mobility of cells on protein-containing SLBs. This increases the number of cell-cell contacts and therefore improves cell vitality and network formation. On the contrary, substrates with a high surface charge such as PDL+laminin can reduce cell mobility and therefore hinder network formation.

### 3.3. Co-localization of ephrinA5-Fc and EphrA5 receptor

The neuronal attachment is a crucial event in regulating and initiating the neural growth and maturation. In this regard, the EphrA-associated kinase domain mediates signaling cascades by phosphorylation of tyrosine residues. Activated tyrosine kinases can be found predominantly at axons and dendrites.<sup>10</sup> In this study, we

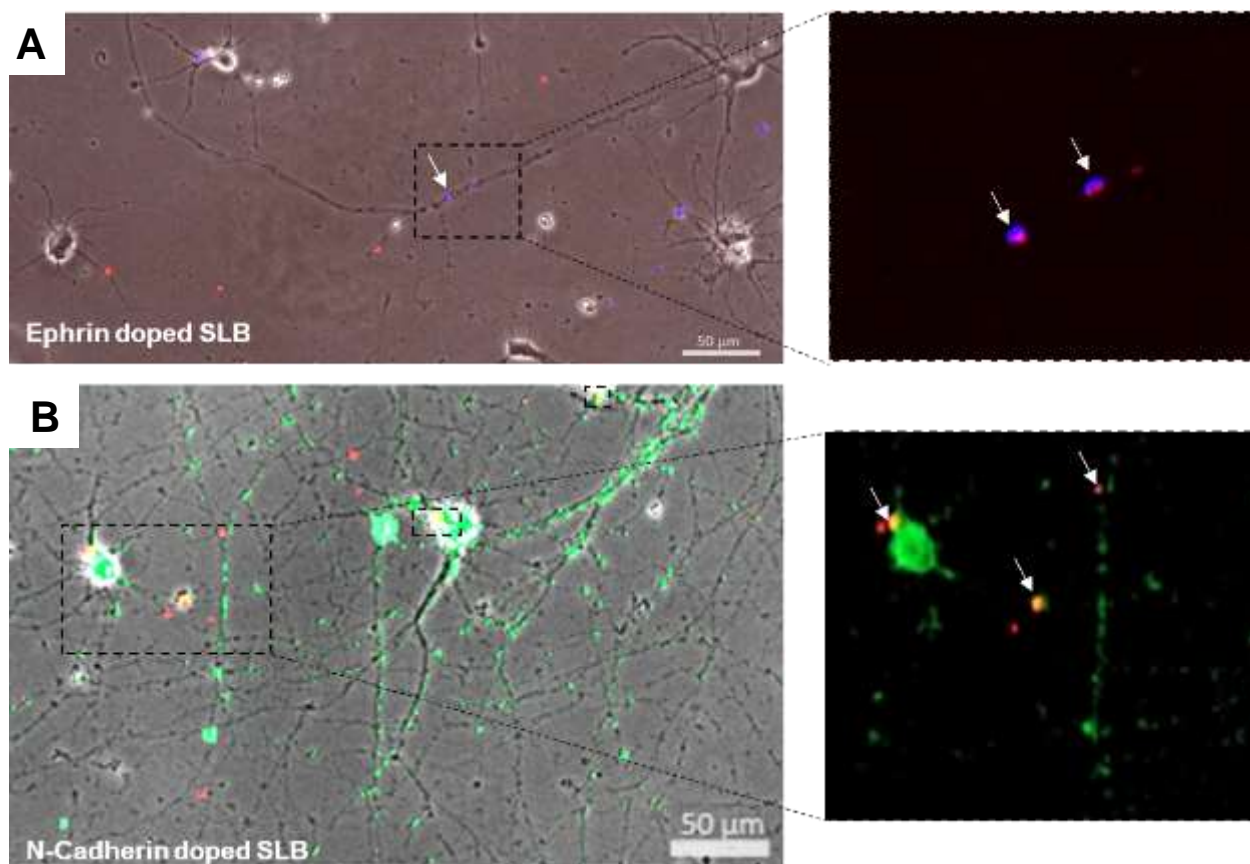


**Figure 4:** Co-localization of bilayer incorporated and native protein during cortical neuron adhesion on a SLB (DIV14). **A)** Interaction of ephrinA5-Fc (red, DyLight594) and EphrA receptor (mouse anti-rat EphrA5, blue, AlexaFluor 350) along axons and dendrites of cortical neurons. **B)** Homophilic interaction of N-cadherin proteins. Co-localization (yellow) of membranous N-cadherin (green, AlexaFluor 488) and N-cadherin-Fc (red, DyLight 594). Scale bar 50  $\mu\text{m}$ .

performed immunofluorescence analysis to investigate the improved neuronal adhesion due to the binding between ephrinA5 that was incorporated in lipid membranes (Figure 4 A). To determine the functional co-localization of ligand-receptor interactions, ephrinA5 was labeled prior to incorporation in lipid vesicles with DyLight 594 to exclude endogenously expressed or secreted ephrinA5 from the images. Endogenous EphrA were immunolabeled and imaged using AlexaFluor 350. The co-localization of incorporated ephrinA5 and EphrA can be seen in Figure 4A, inset. Immunofluorescence analysis confirms a specific interaction of EphrA5-R (blue, AlexaFluor 350) and ephrinA5-Fc protein (red, DyLight 594) and reveals that the active ephrin protein domain remains accessible on the surface of the SLB (Figure 4, A inset). Additionally, these findings support that ephrinA5 is precisely anchored in the lipid membrane implying that the Fc-chimera of ephrinA5 are exhibiting the right orientation to enable biologic activity. Control conditions have shown that a bare POPC lipid membrane does not show any cell adhesion (S2, Supplementary information). Ghosh Moulick et al. described that addition of EphrA5 after formation of ephrinA5-Fc doped POPC lipid membranes did not support an attachment of cortical neurons, confirming a proper orientation of ephrinA5-Fc and functional activation of the appropriate EphrA5.<sup>32</sup> Only a correct anchoring to ephrinA5 on the lipid bilayer with the possibility to change the protein orientation can provide cell adhesion and support neural network formation. Moreover, ephrinA5 is predominantly localized at axons as well as neurites, which exemplifies the importance of ephrinA5 in neurite guidances.<sup>10</sup> Especially, the anchorage and outgrowth of neurites on ephrinA5-Fc doped SLBs can be confirmed in this current study. The accumulation of ephrinA5-Fc (red, DyLight594) and EphrA5 (blue, AlexaFluor350) on neurites are highlighted as white arrows (Figure 4A, magnification).

### 3.4. Co-localization of N-cadherin

N-cadherin is a calcium-dependent adhesion molecule which associates with  $\alpha$ - and  $\beta$ -catenin and regulates multiple processes including embryonic development.<sup>39,40</sup> During late development, N-cadherin's expression is focused predominantly at excitatory neuronal terminals.<sup>41</sup> To determine the functional co-localization of N-cadherin, N-cadherin-Fc was labeled prior to incorporation in lipid vesicles with DyLight 594 to exclude membranous or secreted N-cadherin. Membranous N-cadherin was immunolabeled and imaged using AlexaFluor 488. The co-localization of dimerized N-cadherin proteins is visualized in Figure 4. The co-localization of incorporated N-cadherin and membranous N-cadherin has shown that the interaction occurs preferentially on neurites as well as in the close proximity to the cell body of cortical neurons (yellowish, overlay of labeled N-cadherin-Fc (DyLight 594) and membranous N-cadherin (Figure 4, B inset)). Similar to EphrA5-R and ephrinA5-Fc interactions, this result supports the concept that a correct anchoring of the N-cadherin-domain to membranous N-cadherin protein occurred (Figure 4, B inset, co-localization of homophilic binding, yellow). Okada et al. reported that N-cadherin in neural cells are recruited to activated synapses and preferentially exists at spines where they maintain spine stability.<sup>15</sup> In our study we could show that N-cadherin dimerization occurs at neurites and is localized at the cell soma. The attachment of N-cadherin to activated synapses has to be further analyzed.

### 3.5. Synaptophysin expression in cortical neurons on lipid bilayer

Primary neuronal culture is a powerful tool to investigate cellular and molecular mechanisms of neuronal development, aging, and death. Cell culture model systems are used to further understand these mechanisms as well as neural dysfunction or even degeneration. To investigate the progression of primary isolated neurons to a tissue with mature network architecture, we cultivated E18 cortical neurons on human synaptic recombinant proteins, here ephrinA5 and N-cadherin, to assess the early stages of neural maturation. Here, we studied the expression of synaptophysin by immunofluorescence analysis (Figure 5). Synaptophysin is a 38 kDa glycoprotein which belongs to a structural element of the walls of synaptic vesicles<sup>42,43</sup> and acts as a positive marker of neuronal maturation in late neuronal differentiation,<sup>44</sup> a central role in synaptogenesis. The development of neuronal networks and the expression of synaptophysin expression was monitored on poly-D-Lysine coated surfaces (Figure 5, i-ii'), as well as on ephrinA5- and N-cadherin-doped lipid bilayers (Figure 5, iii - vi').

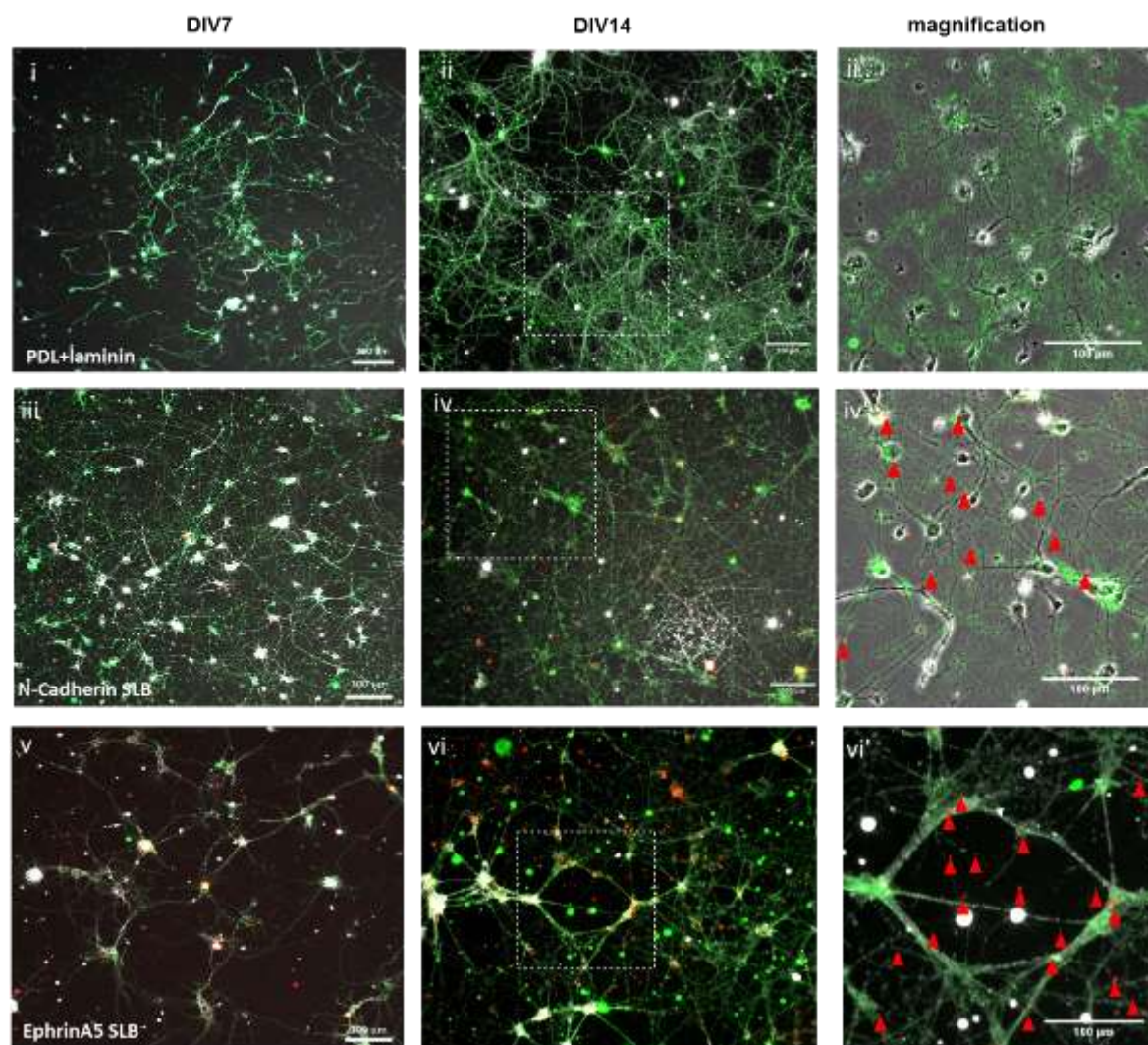


**Figure 5: Maturation-related targeting of synaptophysin in cortical neurons.** Neurons are labeled against TUJ1 (white), and synaptophysin (green) in i-vi' at DIV7 and DIV14. Synaptophysin expression in neuronal cells is shown on (i) PDL+laminin coating, (iii) N-cadherin lipid bilayer, and (v) ephrinA5 lipid bilayer. Red arrows indicate the localization of SLB incorporated proteins. Scale bar represents 100  $\mu\text{m}$ .

Immunocytochemistry of cortical neurons on PDL+laminin substrates (i-ii'), N-cadherin- (iii-iv') and ephrinA5 (v-vi')-doped lipids at DIV7 reveal a distinct synaptophysin expression. Immunofluorescence microscopy analysis has shown that cortical neurons extend prominent neurites at DIV7 on PDL+laminin surfaces and N-cadherin-modified lipid bilayers (i and iii), while cortical neurons on ephrinA5-modified lipid bilayers produce cell clusters connected by shortened neurites. Here, the network formation is insufficiently developed at DIV7 (v). Cortical cultures on PDL+laminin substrates show developed neural network with synaptic junctions (Figure 5, ii), whereas cortical neurons on N-cadherin lipid bilayers show an extensively developed finely meshed neural network architecture (Figure 5, iv). As cortical neurons mature and form synapses, synaptophysin is preferentially localized on neurites (Figure 5, iv'). TUJ1 staining confirms the presence on dendritic and axonal junctions. By DIV14, many synapses were found in cortical neurons on PDL+laminin surfaces and N-cadherin lipid bilayers (Figure 5, ii - ii' and iv - iv'). On these substrates, dendrosynaptic and axosomatic synapses (presynapses localized around the soma) have been extensively developed. Cortical neurons on ephrinA5 lipid bilayers

show a very low synaptophysin expression, constrained mainly to cell aggregates (Figure 5, vi') in agreement with the reduced structural maintenance of the network architecture on ephrinA5 (white arrows, vi'). EphrinA5-Fc proteins are predominantly gathered by cells from the SLB and localized to the soma (Figure 5, v and vi') and are located on dendrites or axons (vi).

A weak expression of synaptophysin in immature synapses of cortical neurons on PDL coated surfaces at DIV5 has been previously demonstrated by Suisse and Martin (2002) but the development of nascent synaptic connections was present. Cultivation of the cortical neurons to DIV15-DIV20 led to the highest synaptophysin expression level and a matured phenotype.<sup>45</sup> This is consistent with our findings on PDL+laminin substrates. In mature neurons, synaptophysin has a prominent presence in presynaptic axon terminals and along dendrites,<sup>45</sup> as can also be observed in our findings for cortical neurons at DIV14 on PDL+laminin (ii'). In contrast, cortical neurons on N-cadherin lipid bilayers already show a level of synaptophysin expression at DIV7 that is comparable to what is seen in cortical cultures on PDL+laminin substrates at DIV14. We therefore assume that cortical neurons on N-cadherin lipid bilayers mature earlier than

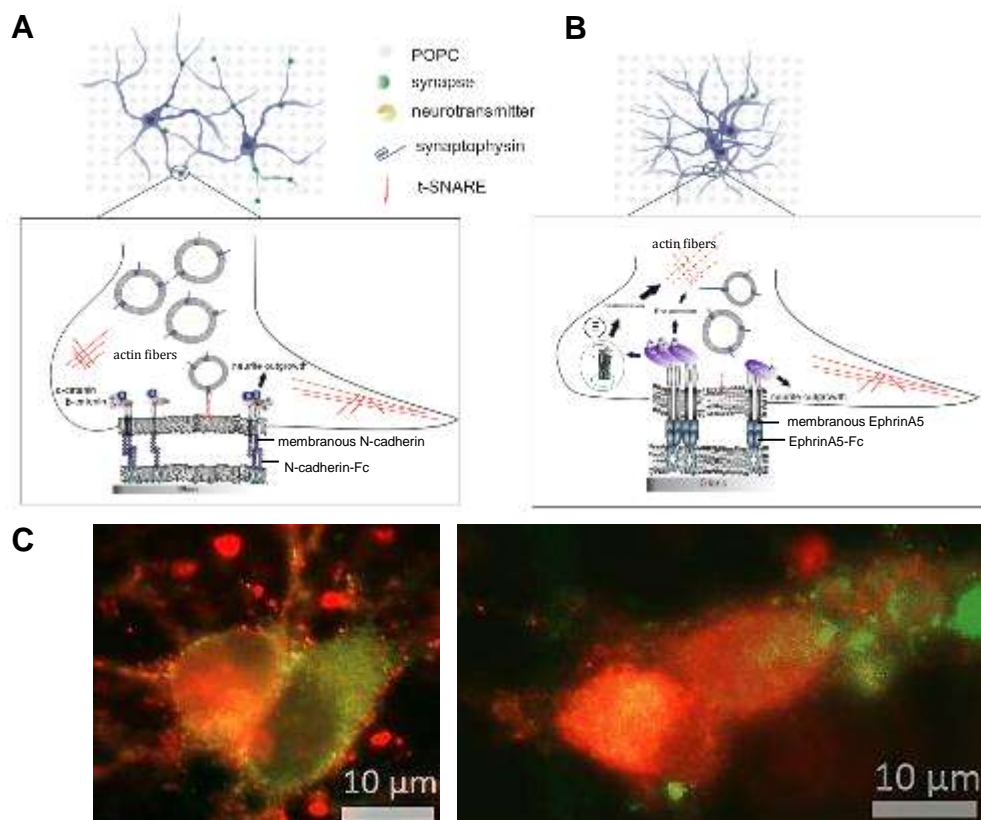


**Figure 6: Adhesion mechanism of cortical neurons on modified lipid membranes.** A) Schematic representation of cell adhesion and maturation of neuronal cells via homophilic interaction of N-cadherin in the cell membrane with N-cadherin-Fc in the SLB and associated neurite formation.  $\alpha$ -catenin,  $\beta$ -catenin linked to tyrosine kinase; P: phosphorylated; B) Schematic illustration of cell adhesion via EphrA receptors to SLB-incorporated ephrinA5-Fc. Interactions of ephrinA5-Fc and EphrA receptor after endocytosis triggers changes in neurite outgrowth. E: Endocytosis of EphrA receptor-ligand complex. C) Immunocytochemistry of co-expressed phosphorylated tyrosine kinases, (PY-99, red) in cortical neurons after DIV7 on N-cadherin and ephrinA5 doped lipid bilayers. Endogenously expressed EphrA receptor and N-cadherin are visualized in green. Scale bar 10  $\mu$ m.

on PDL+laminin substrates or ephrinA5 lipid bilayers. This is emphasized by the fact that the detected N-cadherin-Fc proteins are predominantly restricted to neurites identified as fine red dots (Figure 5, iv'). Fletcher et al. described that action potential-stimulated neurons and the precise localization of N-cadherin on synapses are in close relationship to pre- and postsynaptic marker components, such as synaptophysin and the post-synaptic density protein-95 (PSD-95).<sup>46</sup> The dynamics and the response of synapses are known to be mediated by N-cadherin's presence. Furthermore, N-cadherin causes vesicle fusion at the presynaptic membrane<sup>47</sup> that we assume, that incorporated Fc-N-cadherin trigger the appearance of synaptic junction complexes in cortical neurons in contrast to incorporated ephrinA5 (Figure 6, A). We could preferentially detect less synaptophysin in cells close to their neighbor cell's soma and occasionally localized on shortened neurites at DIV14. We assume that neurons develop fewer synapses on ephrinA5 in the first seven days due to a clustering of cells resulting in fewer attachment sides and a weak neural network formation (based on Figure 5, v). We propose that the accumulation of EphrA receptors (Figure 6 B) induces a destabilizing effect on the actin cytoskeleton by a high phosphorylation of the downstream kinase, resulting in neuronal detachment and reduction of synaptophysin. Further immunostaining analyses of co-expressed phosphorylated tyrosine (PY-99, red) in cortical neurons with co-localized N-cadherin or ephrinA5 are shown in Figure 6, C. The analyses confirm that the tyrosine kinase (PY-99) in cortical cells is highly regulated by ephrinA5 and N-cadherin-Fc doped SLBs (Figure 6, C). The influence of N-

cadherin- or ephrinA5-doped SLBs on the phosphorylation of p-Tyr and the activation of downstream signaling cascades should be further investigated by western blot analysis.

### 3.6. Calcium imaging analysis

Calcium imaging was employed to measure spontaneous neuronal activity on the substrates. Neurons were cultured on lipid membranes for up to DIV14 and exhibited spontaneous activity throughout the entire population. The propagation of signals among adjacent neurons was detected by optical recordings of calcium influx during action potentials. Changes in intracellular calcium concentration were visualized by changes of fluorescence intensity in the calcium sensitive dye Fluo-4. Subsequently, intensity analysis was performed using a MatLab analysis software developed in-house. Regions of interest (ROIs) for intensity analysis were selected manually with the Zeiss ZENblue Software. All measurements were performed at either DIV7 (P=10, n=3) or DIV14 (P=10, n=3) for each substrate type and age.

The development of spontaneous activity in neuronal cells is dependent on neural adhesion proteins. Dissociated cortical neurons mature on PDL+laminin at DIV14 to DIV21 and show an elaborated plexus of axons, dendrites, and synapses with well-developed neuronal morphology (data not shown). Our findings reveal that the percentage of active neurons on PDL+laminin coated substrates and lipid bilayers doped with synaptic adhesion proteins varies drastically at DIV7 and DIV14. Here, we could demonstrate that the percentage of active neurons sharply increased on N-cadherin-doped lipid bilayers until DIV7 and remained at a high level of activity through DIV14. In contrast, the percentage of active neurons on PDL+laminin substrates and ephrinA5 lipid bilayers slowly increased over time until DIV14 (Figure 7, A) though exhibiting a markedly lower level of activity as compared to neurons on N-cadherin-doped bilayers throughout the experiment. Based on immunostaining analysis of synaptophysin and evaluation of the neurite length over time on different substrates, we hypothesize in our study that neurons grown on N-cadherin lipid bilayers show earlier spontaneous activity in comparison to PDL+laminin-coated surfaces or even ephrinA5-doped lipid bilayers, as can be seen in the calcium imaging measurements (Figure 7, B). These findings obtained from calcium analysis confirm that the majority of neurons on N-cadherin-doped lipid bilayers exhibit spontaneous activity at DIV7. Here, the high amount of intracellular calcium in cortical cells grown on N-cadherin-doped

SLBs is reflected in high firing amplitudes with five regular bursts in 6 ms. In contrast, neurons grown on ephrinA5 SLBs show a lower fluorescence with eight irregular bursts in 6 ms. Neurons cultured on PDL+laminin show the same firing amplitude as neurons on ephrinA5 SLBs, but exhibit only two bursts in 6 ms with a delay of 3 ms. Here, the amount of calcium present in neurons on ephrinA5 SLBs and on PDL+laminin substrates is three times lower than in neurons grown on N-cadherin SLBs. At DIV14, neurons on PDL+laminin substrates show a strong fluorescence with five sequential strong bursts in 6 ms, whereas neurons on N-cadherin SLBs exhibit a strong long-lasting burst of about 2 ms. Neurons on ephrinA5 SLBs show a fluorescence change of less than 10% with sequential bursts with an interval of 1 ms. The amount of calcium present in neurons on ephrinA5 SLBs is five times lower than in neurons grown on PDL+laminin or N-cadherin SLBs.

Fluorescence analysis displays a fast onset due to neuronal activation, followed by decay back to the baseline in neuronal cultures on N-cadherin SLBs at DIV7 and DIV14 and PDL+laminin substrates at DIV14. The burst dynamics of neurons on ephrinA5 SLBs at DIV7 are low. Furthermore, the presence of detectable bursts is sparse, the burst timing is irregular, and the firing amplitudes are low. Also, the shape and strength of a burst did not increase and the bursting does not become more regular.

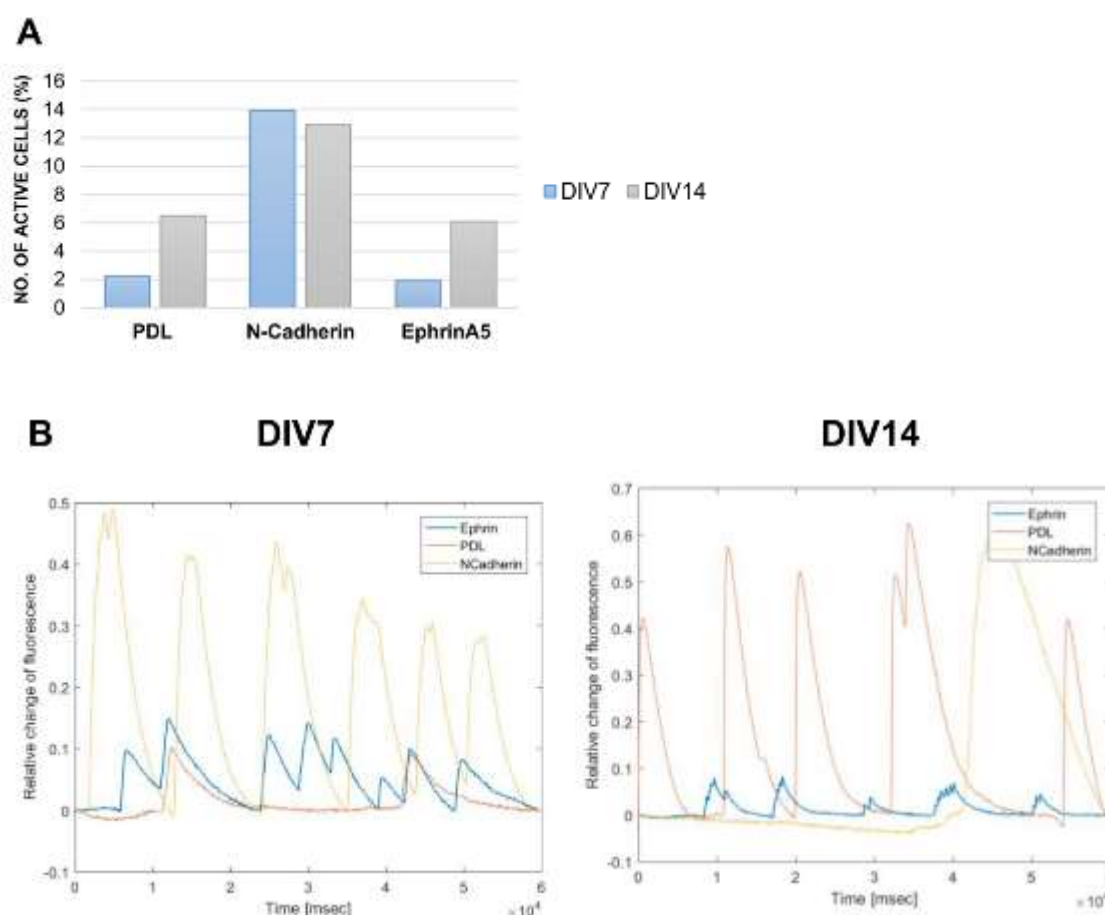


**Figure 7: Analysis of neuronal activity on artificial lipid membranes.** Representative fluorescence traces of average network activity on different substrates. A. Analysis of active cells on PDL+laminin substrates, N-cadherin, or ephrinA5 lipid membranes indicate that, in contrast to neurons on ephrinA5 membranes or PDL+laminin substrates, neurons on N-cadherin membranes already show a high neural activity at DIV7. B) Relative change in fluorescence intensity of active cells on PDL+laminin substrates or artificial membranes with N-cadherin or ephrinA5 at DIV7 and DIV14. Calcium imaging indicates a strong activity of neurons on N-cadherin lipid bilayers at DIV7.

It is noticeable that the network's dynamic behavior changes over time. At DIV14 neurons on PDL+laminin show a strong fluorescence with five regular strong bursts, whereas neurons on N-cadherin SLBs exhibit fewer bursts with a strong long-lasting action potential, during which the increase in fluorescence is similar to the one observed for neurons on PDL+laminin substrates but with an irregular firing rate.

Neuronal network activity in cultures is characterized by episodes of bursts, where neurons fire in a synchronized manner in a short time windows of ~200ms. The properties of spontaneous activity depends on the excitability of the neuron and the connectivity of the neuronal network. In this case, the accessibility to recruit, transfer, amplify, and propagate the activity to their adjacent cells.<sup>48</sup>

Neurons in our preparations are plated homogeneously on PDL+laminin substrates to develop a neural network, which is electrically excitable by DIV14. With our new approach and the use of artificial membranes, we could show that incorporated N-cadherin plays an important role in neural network connectivity and circuitry. We found that N-cadherin increases the neural connectivity by eliciting earlier spontaneous activity with regular burst timing and firing amplitudes already at DIV7, which is supported by previous analysis in this study showing well-developed synaptic junctions resulting in an earlier neuronal activity.

#### 4. Conclusions

We reported the establishment of artificial membranes with incorporated synaptic adhesion proteins and their effect on the neural attachment, network formation, and neural stimulation. In this approach using ephrinA5 or N-cadherin Fc-chimera proteins, we studied the interaction of endogenous neural receptors with their Fc-chimera ligands on neural development. Here, synaptic adhesion proteins or PDL have shown that the adhesion is dependent on the adhesive specificity. In accordance with the adhesion studies, we observed a high phosphorylation state of the receptor tyrosine kinase for N-cadherin- or ephrinA5-doped lipid bilayers. N-cadherin-modified lipid bilayers showed the highest neural activity by calcium imaging analysis at DIV7 as well as a higher expression of synaptophysin, which results in earlier neuronal activity. Our results indicate an improvement of neural adhesion, neurite extension, and maturation by the use of Fc-chimera N-cadherin anchored to lipid membranes at DIV7, in contrast to PDL+laminin substrates or recombinant Fc-chimera ephrinA5 proteins. The lack of longlasting adhesion of neurons on ephrinA5-doped lipid membranes leads to the conclusion that ephrinA5 clustering results in a destabilization of the neural adhesion by decreasing cell-substrate contact points. As a consequence, cell clustering occurred early in cell cultivation. The presented system of Fc-chimera proteins incorporated into SLBs provides a new possibility to incorporate synaptic adhesion proteins in a fluid membrane allowing good accessibility to cells. Furthermore, we propose our system as an applicable and adaptable tool for the incorporation of further Fc-chimera modified proteins of interest, which set a new concept in fabricating immunosensors or neuronal recording devices.

#### Conflicts of interest

There are no conflicts of interest to declare

#### Acknowledgements

The authors would like to thank Bettina Breuer, Rita Fricke and Dr. Vanessa Maybeck for their support in providing primary

cortical neurons. Eleonora Quiroli for her work on the analysis of neuronal activity on artificial lipid membranes and Corinna Meeßen for providing a MatLab script for the calcium analysis. Dr. Vanessa Maybeck and Sabrina Weidlich are acknowledged for proofreading the manuscript.

#### References

1. M. B. Dalva, A. C. McClelland and M. S. Kayser, *Nat Rev Neurosci*, 2007, **8**, 206-220.
2. M. Missler, T. C. Sudhof and T. Biederer, *Cold Spring Harb Perspect Biol*, 2012, **4**, a005694.
3. T. C. Sudhof, *Nature*, 2008, **455**, 903-911.
4. A. K. Majewska, J. R. Newton and M. Sur, *J Neurosci*, 2006, **26**, 3021-3029.
5. P. Suetterlin, K. M. Marler and U. Drescher, *Semin Cell Dev Biol*, 2012, **23**, 1-6.
6. K. K. Murai and E. B. Pasquale, *J Cell Sci*, 2003, **116**, 2823-2832.
7. J. G. Flanagan and P. Vanderhaeghen, *Annu Rev Neurosci*, 1998, **21**, 309-345.
8. A. Davy, N. W. Gale, E. W. Murray, R. A. Klinghoffer, P. Soriano, C. Feuerstein and S. M. Robbins, *Genes Dev*, 1999, **13**, 3125-3135.
9. A. Davy and S. M. Robbins, *EMBO J*, 2000, **19**, 5396-5405.
10. M. Reber, R. Hindges and G. Lemke, *Adv Exp Med Biol*, 2007, **621**, 32-49.
11. Y. Akaneya, K. Sohya, A. Kitamura, F. Kimura, C. Washburn, R. Zhou, I. Ninan, T. Tsumoto and E. B. Ziff, *PLoS One*, 2010, **5**, e12486.
12. C. Luccardini, L. Hennekinne, L. Viou, M. Yanagida, F. Murakami, N. Kassar, X. Ma, R. S. Adelstein, R. M. Mege and C. Metin, *J Neurosci*, 2013, **33**, 18149-18160.
13. Y. Yang, X. B. Wang, M. Frerking and Q. Zhou, *J Neurosci*, 2008, **28**, 5740-5751.
14. P. Mendez, M. De Roo, L. Poglia, P. Klauser and D. Muller, *J Cell Biol*, 2010, **189**, 589-600.
15. D. Okada, F. Ozawa and K. Inokuchi, *Science*, 2009, **324**, 904-909.
16. U. Cavallaro and E. Dejana, *Nat Rev Mol Cell Biol*, 2011, **12**, 189-197.
17. M. Overduin, T. S. Harvey, S. Bagby, K. I. Tong, P. Yau, M. Takeichi and M. Ikura, *Science*, 1995, **267**, 386-389.
18. E. Sackmann, *Science*, 1996, **271**, 43-48.
19. T. M. Bayerl and M. Bloom, *Biophys J*, 1990, **58**, 357-362.
20. S. J. Johnson, T. M. Bayerl, D. C. McDermott, G. W. Adam, A. R. Rennie, R. K. Thomas and E. Sackmann, *Biophys J*, 1991, **59**, 289-294.
21. B. W. Koenig, S. Kruger, W. J. Orts, C. F. Majkrzak, N. F. Berk, J. V. Silverton and K. Gawrisch, *Langmuir*, 1996, **12**, 1343-1350.
22. D. Dutta and L. C. Kam, *Methods Cell Biol*, 2014, **120**, 53-67.
23. M. L. Dustin, T. Starr, R. Varma and V. K. Thomas, *Curr Protoc Immunol*, 2007, **Chapter 18**, Unit 18 13.
24. M. Fein, J. Unkeless, F. Y. Chuang, M. Sassaroli, R. da Costa, H. Vaananen and J. Eisinger, *J Membr Biol*, 1993, **135**, 83-92.
25. S. Pautot, H. Lee, E. Y. Isacoff and J. T. Groves, *Nat Chem Biol*, 2005, **1**, 283-289.
26. Q. Xu, W. C. Lin, R. S. Petit and J. T. Groves, *Biophys J*, 2011, **101**, 2731-2739.

27. J. N. Herron, W. Muller, M. Paudler, H. Riegler, H. Ringsdorf and P. A. Suci, *Langmuir*, 1992, **8**, 1413-1416.
28. P. Doherty, P. Smith and F. S. Walsh, *Perspect Dev Neurobiol*, 1996, **4**, 157-168.
29. A. Offenhäusser, S. Bocker-Meffert, T. Decker, R. Helpenstein, P. Gasteier, J. Groll, M. Moller, A. Reska, S. Schafer, P. Schulte and A. Vogt-Eisele, *Soft Matter*, 2007, **3**, 290-298.
30. J. L. Rigaud, B. Pitard and D. Levy, *Bba-Bioenergetics*, 1995, **1231**, 223-246.
31. A. M. Seddon, P. Curnow and P. J. Booth, *Bba-Biomembranes*, 2004, **1666**, 105-117.
32. R. G. Moulick, D. Afanasenkau, S. E. Choi, J. Albers, W. Lange, V. Maybeck, T. Utesch and A. Offenhäusser, *Langmuir*, 2016, **32**, 3462-3469.
33. C. A. Keller and B. Kasemo, *Biophys. J.*, 1998, **75**, 1397-1402.
34. F. C. de Anda, A. Gartner, L. H. Tsai and C. G. Dotti, *Journal of Cell Science*, 2008, **121**, 178-185.
35. A. Gartner, E. F. Fornasiero, S. Munck, K. Vennekens, E. Seuntjens, W. B. Huttner, F. Valtorta and C. G. Dotti, *EMBO J*, 2012, **31**, 1893-1903.
36. J. Egea and R. Klein, *Trends Cell Biol*, 2007, **17**, 230-238.
37. D. J. Marston, S. Dickinson and C. D. Nobes, *Nat Cell Biol*, 2003, **5**, 879-888.
38. M. Zimmer, A. Palmer, J. Kohler and R. Klein, *Nature Cell Biology*, 2003, **5**, 869-878.
39. B. M. Gumbiner, *Nat Rev Mol Cell Biol*, 2005, **6**, 622-634.
40. S. Pokutta and W. I. Weis, *Annu Rev Cell Dev Biol*, 2007, **23**, 237-261.
41. D. L. Benson and H. Tanaka, *J Neurosci*, 1998, **18**, 6892-6904.
42. R. Jahn, W. Schiebler, C. Ouimet and P. Greengard, *Proc Natl Acad Sci U S A*, 1985, **82**, 4137-4141.
43. B. Wiedenmann and W. W. Franke, *Cell*, 1985, **41**, 1017-1028.
44. H. B. Sarnat, *Clin Neuropathol*, 2013, **32**, 340-369.
45. C. Lesuisse and L. J. Martin, *J Neurobiol*, 2002, **51**, 9-23.
46. T. L. Fletcher, P. Cameron, P. De Camilli and G. Banker, *J Neurosci*, 1991, **11**, 1617-1626.
47. H. Tanaka, W. Shan, G. R. Phillips, K. Arndt, O. Bozdagi, L. Shapiro, G. W. Huntley, D. L. Benson and D. R. Colman, *Neuron*, 2000, **25**, 93-107.
48. E. Tibau, M. Valencia and J. Soriano, *Frontiers in neural circuits*, 2013, **7**, 199.